

Cite as: S. M. Reincke *et al.*, *Science* 10.1126/science.abm5835 (2022).

SARS-CoV-2 Beta variant infection elicits potent lineage-specific and cross-reactive antibodies

S. Momsen Reincke^{1,2,3*}†, Meng Yuan^{4†}, Hans-Christian Kornau^{2,5†}, Victor M. Corman^{6,7†}, Scott van Hoof^{1,2,3}, Elisa Sánchez-Sendin^{1,2,3}, Melanie Ramberger^{2,3}, Wenli Yu⁴, Yuanzhi Hua⁴, Henry Tien⁴, Marie Luisa Schmidt⁶, Tatjana Schwarz⁶, Lara Maria Jeworowski⁶, Sarah E. Brandl^{1,2,3}, Helle Foverskov Rasmussen^{1,2,3}, Marie A. Homeyer^{1,2,3}, Laura Stöffler^{1,2,3}, Martin Barner³, Désirée Kunkel⁸, Shufan Huo¹, Johannes Horler^{1,2,3}, Niels von Wardenburg^{1,2,3}, Inge Kroidl^{9,10}, Tabea M. Eser^{9,10}, Andreas Wieser^{9,10}, Christof Geldmacher^{9,10}, Michael Hoelscher^{9,10}, Hannes Gänzer¹¹, Günter Weiss¹², Dietmar Schmitz⁵, Christian Drosten⁶, Harald Prüss^{1,2,3**‡}, Ian A. Wilson^{4,13*‡}, Jakob Kreye^{1,2,3,14*‡}

¹Charité-Universitätsmedizin Berlin, corporate member of Freie Universität Berlin and Humboldt-Universität zu Berlin, Department of Neurology and Experimental Neurology, Berlin, Germany. ²German Center for Neurodegenerative Diseases (DZNE) Berlin, Berlin, Germany. ³Helmholtz Innovation Lab BaoBab (Brain antibody-omics and B-cell Lab), Berlin, Germany. ⁴Department of Integrative Structural and Computational Biology, The Scripps Research Institute, La Jolla, CA 92037, USA.

⁵Charité-Universitätsmedizin Berlin, corporate member of Freie Universität Berlin and Humboldt-Universität zu Berlin, Neuroscience Research Center (NWFZ), Cluster NeuroCure, Berlin, Germany. ⁶Charité-Universitätsmedizin Berlin, corporate member of Freie Universität Berlin and Humboldt-Universität zu Berlin, Institute of Virology, Berlin, Germany and German Centre for Infection Research (DZIF), Berlin, Germany. ⁷Labor Berlin–Charité Vivantes GmbH, Berlin. ⁸Berlin Institute of Health at Charité–Universitätsmedizin Berlin, Flow and Mass Cytometry Core Facility, Berlin, Germany. ⁹Division of Infectious Diseases and Tropical Medicine, Medical Center of the University of Munich (LMU), Germany. ¹⁰German Center for Infection Research (DZIF), partner site Munich, Germany. ¹¹Department of Internal Medicine, BKH Schwaz, Schwaz, Austria. ¹²Department of Internal Medicine II, Medical University of Innsbruck, Innsbruck, Austria. ¹³The Skaggs Institute for Chemical Biology, The Scripps Research Institute, La Jolla, CA 92037, USA. ¹⁴Charité-Universitätsmedizin Berlin, corporate member of Freie Universität Berlin and Humboldt-Universität zu Berlin, Department of Pediatric Neurology, Berlin, Germany.

†These authors contributed equally to this work.

‡These authors contributed equally to this work.

*Corresponding author. Email: momsen.reincke@charite.de (S.M.R.); harald.pruess@charite.de (H.P.); wilson@scripps.edu (I.A.W.); jakob.kreye@charite.de (J.K.)

SARS-CoV-2 Beta variant of concern (VOC) resists neutralization by major classes of antibodies from COVID-19 patients and vaccinated individuals. Here, serum of Beta-infected patients revealed reduced cross-neutralization of wildtype virus. From these patients, we isolated Beta-specific and cross-reactive receptor-binding domain (RBD) antibodies. The Beta-specificity results from recruitment of VOC-specific clonotypes and accommodation of mutations present in Beta and Omicron into a major antibody class that is normally sensitive to these mutations. The Beta-elicited cross-reactive antibodies share genetic and structural features with wildtype-elicited antibodies, including a public VH1-58 clonotype targeting the RBD ridge. These findings advance our understanding of the antibody response to SARS-CoV-2 shaped by antigenic drift with implications for design of next-generation vaccines and therapeutics.

In the course of the COVID-19 pandemic, multiple SARS-CoV-2 lineages have emerged including lineages defined as variants of concern (VOC), such as Alpha (also known as lineage B.1.1.7), Beta (B.1.351), Gamma (P.1), Delta (B.1.617.2) and recently Omicron (B.1.1.529). VOCs are associated with increased transmissibility, virulence, or resistance to neutralization by sera from vaccinated and convalescent individuals who were infected with the original strain (1–7). These distinct lineages carry a variety of mutations in the spike protein, several of which are within the receptor binding domain (RBD), especially at residues K417, L452, T478, E484, and N501. Some mutations like N501Y are associated with enhanced binding to angiotensin-converting enzyme 2 (ACE2), largely driving the global spread of VOCs incorporating these mutations (2). However, with increasing immunity either through natural

infection or vaccination, antibody escape will become more relevant in emerging VOCs. Many studies have investigated RBD antibodies in COVID-19 patients prior to identification of SARS-CoV-2 variants, and we refer to these as wildtype antibodies. Wildtype RBD antibodies revealed a preferential response toward distinct epitopes with enriched recruitment of particular antibody germline genes, where the most prominent were VH3-53 and closely related VH3-66, as well as VH1-2 (8, 9). Structural and functional classification of wildtype RBD mAbs has demonstrated that mAbs from these three enriched germline genes form two major classes of receptor-binding site (RBS) mAbs whose binding and neutralizing activity depends on either K417 or E484 (9, 10). Mutations at these key residues (K417N and E484K) together with N501Y are hallmarks of Beta (2), and largely account for the

reduced neutralizing activity of sera from vaccinated and convalescent individuals against this VOC (1–6, 11, 12). Of the first four VOCs (Alpha through Delta), Beta shows the highest resistance to neutralization by wildtype-elicited sera (12), suggesting conspicuous differences in its antigenicity (13). First reports indicate that Omicron, which shares K417N and N501Y with Beta and carries a different mutation at the third key residue (E484A) as well as 34 further spike mutations, shows even higher resistance to neutralization by wildtype-elicited sera (14). While mutations at position K417 and E484 influence the antigenicity of the RBD, little is known about the antibody response elicited by Beta infection. For example, it is unknown if antibodies targeting the RBD Beta share the preferential recruitment of particular germline genes with wildtype antibodies, and whether VOC-defining mutations K417N and E484K could be accommodated in the canonical binding modes of public antibody classes like VH3-53/VH3-66 antibodies. Thus, we set out to explore genetic, functional, and structural features of the antibody response against RBD in Beta-infected individuals.

We identified 40 individuals infected with SARS-CoV-2 Beta from three metropolitan areas in Germany and Austria (table S1) and collected serum at 38.6 ± 19.2 days after their first positive SARS-CoV-2 RT-PCR test. The patients' IgG bound to wildtype nucleocapsid protein, wildtype spike, or both proteins in 37 of 40 patients, and with stronger reactivity to RBD Beta than to wildtype RBD (fig. S1A). The patients' sera also inhibited ACE2 binding to RBD Beta to a greater extent than to wildtype RBD (fig. S1B and table S1). Reactivity to wildtype spike S1 was confirmed in an additional commercially available ELISA; however, only 23 of 40 samples tested positive according to the manufacturer's cutoff (fig. S1, C and D). In a plaque reduction neutralization test (PRNT), 37 of 40 sera neutralized an authentic SARS-CoV-2 Beta isolate with a half-maximal inhibitory concentration (IC_{50}) at 1:20 dilution or greater (Fig. 1A). In contrast, only 11 of 40 sera neutralized wildtype virus (Fig. 1B). The neutralizing activity against the two isolates was modestly correlated (fig. S1E), with a ~20-fold reduction of neutralizing activity against wildtype virus compared to Beta (Fig. 1C and fig. S1F). A converse effect has been reported after immune responses against wildtype RBD in convalescent and vaccinated individuals (2), where neutralization of SARS-CoV-2 Beta was ~8- to ~14-fold reduced compared to wildtype virus (1–6). No positive correlation was found between neutralizing antibodies against Beta and the timepoint of sample collection relative to first positive PCR test (fig. S1G). Neutralizing antibodies against Beta modestly correlated with age (fig. S1H), but no statistically significant gender difference was observed (fig. S1I). Collectively, these data show that sera from Beta-infected patients exhibit reduced cross-reactivity to wildtype SARS-CoV-2, therefore impacting diagnostic antibody testing when using wildtype antigens and adding complexity to the concept of defining a threshold for protective antibody titers.

To investigate the effect of this difference in reactivity between RBD Beta and wildtype RBD at the level of mAbs elicited by SARS-CoV-2 Beta infection, we isolated CD19⁺CD27⁺ memory B cells from the peripheral blood of 12 donors in our cohort by fluorescence activated cell sorting using a recombinant RBD Beta probe (fig. S2, A and B). Using single-cell Ig gene sequencing (15, 16), we derived 289 pairs of functional heavy (IGH) and light (IGL) chain sequences from IgG mAbs (table S2). Sequence analysis showed enrichment of certain genes compared to mAbs derived from healthy, non-infected individuals, including VH1-58, VH3-30, VH4-39 and VH3-53, illustrating a preferential recruitment of certain VH genes (Fig. 2A), VH-JH gene combinations (fig. S3A), and variable light chain genes (fig. S3B). For some genes like VH1-58 and VH3-53, enrichment has previously been identified in CoV-AbDab, a database of published SARS-CoV-2 mAbs (9, 17). We confirmed this finding for all human wildtype RBD mAbs in CoV-AbDab (Fig. 2A). Consistent with reports from wildtype SARS-CoV-2 infections (18–20), the somatic hypermutations (SHM) count was generally low in mAbs of our cohort (fig. S3C). Together, these findings argue for conservation of certain antibody sequence features between antibody responses in different donors and between antibody responses elicited against Beta and wildtype virus. Hence, we compared antibody sequences after Beta infection to all previously published wildtype RBD mAbs and identified several clonotypes shared between both datasets (Fig. 2B), some of which were present in multiple patients of our study (Fig. 2C). Thus, a subset of the antibodies to RBD Beta and wildtype RBD converge on recruitment of specific germline genes.

However, other gene enrichments found in our study like VH4-39 have not been identified within the CoV-AbDab mAbs (Fig. 2A) (9), exemplifying concurrent divergence in the antibody response to the different RBDs. Strikingly, VH1-2, one of the most common genes contributing to the RBD antibody response to wildtype SARS-CoV-2, was drastically reduced in our dataset (Fig. 2A and table S2), consistent with the dependence of VH1-2 mAbs on E484 (9). VH3-53/VH3-66 antibodies bind to wildtype RBD in two canonical binding modes, which involve residues K417 and E484, respectively; binding and neutralization of these antibodies are strongly affected by the K417N and E484K mutations in RBD Beta (9, 21). We therefore hypothesized a similarly reduced recruitment of VH3-53/VH3-66 mAbs after Beta infection. Surprisingly, we identified 15 VH3-53/VH3-66 mAbs, albeit at a reduced frequency compared to the CoV-AbDab dataset (4.7% vs. 19.4%), but still at an increased frequency compared to healthy donors (Fig. 2A), thus indicating either a non-canonical binding mode or accommodation of these mutations into the known binding modes.

To determine the binding properties of antibodies elicited by SARS-CoV-2 Beta, we selected representative mAbs for expression (table S2). We identified 81 mAbs with strong binding to RBD Beta (table S3). Of those, 44 revealed comparable binding to

wildtype RBD and were considered cross-reactive mAbs, whereas 37 mAbs did not bind wildtype RBD and were considered Beta-specific. There were no differences in V gene SHMs, CDR H3/L3 hydrophobicity, and ACE2 binding inhibition between Beta-specific and cross-reactive antibodies (fig. S4, A to C), but the cross-reactive antibodies had a slightly shorter CDR H3/L3, and lower isoelectric point of their CDR H3 (fig. S4, D and E). The neutralization potencies were similar between Beta-specific and cross-reactive mAbs (fig. S4F). Interestingly, all Beta-specific VH3-30 mAbs paired with JH6 (fig. S4G), whereas all cross-reactive VH3-30 mAbs paired with JH4 (fig. S4H). Competition experiments showed that many of the strongly neutralizing Beta-elicited mAbs compete for RBD binding (fig. S4I), indicating that they target similar epitopes.

Next, we aimed to determine the residues that define the binding selectivity for the 37 RBD Beta-specific mAbs and performed ELISAs with single mutant constructs of RBD Beta and wildtype RBD. For all three Beta-defining RBD mutations (K417N, E484K and N501Y), we identified mAbs with RBD binding that depended on a single residue. The Beta-specificity of the other mAbs was dependent on multiple residues (Fig. 3A). RBD Beta-specific mAbs were encoded by diverse VH genes (Fig. 3A and table S2), and 26 of the RBD Beta-specific mAbs (70.2%) neutralized the authentic SARS-CoV-2 Beta isolate (Fig. 3A). Interestingly, all nine Beta-specific VH4-39 mAbs from three different patients were Y501-dependent, comprising 81.8% of all Y501-dependent mAbs. This finding suggests a common binding mode of these clonally unrelated mAbs that depends on Y501, a residue present in RBD Beta, Alpha, Gamma and Omicron, but not Delta, and may explain the frequent use of VH4-39 in mAbs to RBD Beta (Fig. 2A). VH4-39 Y501-dependent mAbs revealed few SHM in VH genes but no uniform pattern in other sequence features (fig. S5A). Although all VH4-39 RBD Beta-specific mAbs bind to a Y501-dependent epitope, their neutralization activity showed noticeable differences (IC_{50} ranging from 5.2 to 947 ng/ml, fig. S5B). Surface plasmon resonance measurements of these mAbs to RBD Beta revealed equilibrium dissociation constants (K_d) between 3.39 and 80.4 nM (fig. S5C) with correlation to their PRNT-derived IC_{50} values (fig. S5D), thereby providing an explanation for the variability in neutralizing activity within the VH4-39 Y501-dependent mAbs.

Furthermore, we identified three VH3-53/VH3-66 mAbs with RBD Beta specificity that all showed neutralizing activity. To determine whether this RBD Beta specificity results from a non-canonical binding mode or accommodation of Beta-defining mutations in one of the two main VH3-53/VH3-66 mAb binding modes, we determined a crystal structure of VH3-53 antibody CS23 in complex with RBD Beta. VH3-53/VH3-66 mAbs with short CDRs H3 (<15 amino acids) target the RBS of wildtype RBD through a canonical mode (10, 22–25) that is highly sensitive to the K417N mutation (9). CS23 contains a CDR H3 with only ten

amino acids and is specific to N417 RBDs including RBD Beta (Fig. 3A). However, CS23 binds to RBD Beta in the canonical mode, with a nearly identical approach angle compared to wildtype VH3-53 antibody CC12.3 (Fig. 3B) (24). We previously showed that the CDR H1 ³³NY³⁴ and H2 ⁵³SGGS⁵⁶ motifs of VH3-53/VH3-66 mAbs are critical for RBD recognition (24). Here we find that CS23 retains these motifs and they interact with the RBD in the same way (Fig. 3, C and D). Residues in CDR H3 usually interact with K417 and thus confer specificity to the wildtype RBD (9). For example, V_H D97 of CC12.1 forms a salt bridge with the outward facing RBD-K417, whereas V_H F99 and V_H G97 of CC12.3 interact with K417 through cation-π and hydrogen bonds (H-bonds), respectively (Fig. 3, E and F). Instead, in RBD Beta, the shorter N417 flips inward and H-bonds with RBD-E406 and Q409 (Fig. 4G). V_H M98 occupies the vacated space and interacts with RBD-Y453, L455, and V_L W91 in a hydrophobic pocket. Modeling shows that K417 would be unfavorable for RBD binding to CS23 (fig. S6A). CDR H3 contains a V_H ⁹⁶TAMA⁹⁹ sequence that forms an ST motif that stabilizes CDR H3 and the orientation of M98. The first serine (S) or threonine (T) residue in a four or five residue ST motif makes two internal H-bonds from the side-chain oxygen of residue i to the main-chain NH of residue i + 2 or i + 3, and between the main-chain oxygen of residue i and the main-chain NH of residue i + 3 or i + 4. In this case, the T96 side chain H-bonds with the main-chain NH of M98, and the T96 main-chain oxygen H-bonds with the main-chain NH of A99 (fig. S6A). This V_H ⁹⁶TxMx⁹⁹ motif is different from all known CDRs H3 of anti-RBD VH3-53/VH3-66 antibodies (17) and explains the newly acquired specificity of this VH3-53 antibody for an RBD with N417. Previously, wildtype VH3-53 antibody COVOX-222 was shown to cross-react with RBD Beta despite interacting with K417 and N501, but nevertheless binds the RBD in the canonical mode; in this case, a rare SHM V_L S30P mutation accommodated Y501 (1) (fig. S6, B and C). Likewise, for CS23, the CDR L1 ³⁰SK³¹ dipeptide is mutated to ³⁰GQ³¹ and accommodates Y501 in Beta (fig. S6D). Interestingly, another VH3-53 antibody of our cohort, CS82 is highly cross-reactive and binds SARS-CoV (Fig. 4A), which was not known for any previous VH3-53 antibodies. CS82 competes with CR3022, which binds to a lateral face of the RBD outside the RBS (fig. S6E), and might suggest a possible alternative binding mode or orientation compared to the two previously identified binding modes of wildtype VH3-53 antibodies that are usually sensitive either to K417N or to E484K (23, 24). Collectively, VH3-53/VH3-66 mAbs contribute to the immune response to RBD Beta with mAbs that accommodate Beta-specific mutations into canonical modes and by mAbs that may bind in alternative binding modes.

We next aimed to characterize the functional breadth of the cross-reactive mAbs. 20 of the 44 cross-reactive mAbs (45.5%) neutralized authentic SARS-CoV-2 Beta isolate (Fig. 4A). To investigate their cross-reactivity against further RBD variants, we performed ELISAs with RBD constructs of VOCs Alpha through Delta

and SARS-CoV. Whereas only two mAbs (10%) strongly detected SARS-CoV RBD, the majority of cross-reactive antibodies bound the RBD of Alpha, Gamma and Delta (Fig. 4A). In PRNT assays with further authentic virus isolates, 15 (75%) Beta neutralizing cross-reactive mAbs also neutralized wildtype virus and 14 (70%) neutralized a Delta virus isolate, which of the VOCs was the most antigenically distinct from the others at the time of testing (Fig. 4A). Six cross-neutralizing antibodies were encoded by VH1-58 (Fig. 4A). VH1-58 is the most enriched germline VH gene in RBD antibodies in both Beta and wildtype infection (26) (Fig. 2A). VH1-58 RBD antibodies almost exclusively pair with JH3 (fig. S3A). This VH1-58/JH3/VK3-20/JK1 clonotype has been described in individuals infected with wildtype virus (20, 26) and found in several patients within our cohort (Fig. 2C and table S6), thereby representing 2.4% of all Beta-elicited IgG mAbs analyzed in this study (table S2). To elucidate the structural basis of this public broadly reactive clonotype, we determined crystal structures of CS44 and CV07-287, a mAb of the same clonotype that was isolated from a wildtype-infected individual (19), in complex with RBD Beta and wildtype RBD respectively (Fig. 4B). We compared the structures of CS44 and CV07-287 with other published VH1-58 antibodies, including COVOX-253 (27), S2E12 (28), A23-58.1, and B1-182.1 (26). These antibodies all target the RBD in the same binding mode (Fig. 4B), which suggests that this public clonotype is structurally conserved. The dominant interaction of VH1-58 antibodies is with the RBD ridge region (residues 471–491), which accounts for ~75% of the entire epitope surface. Most of the VOC mutations occur outside of the ridge region (e.g., residues 417, 452, and 501) and are distant from the binding sites of VH1-58 antibodies CV07-287 and CS44 (Fig. 4, C and D). Among the VOC-related residues, only T478 interacts with VH1-58 antibodies, but mutation to a lysine can be accommodated (Fig. 4A) (26). V_H W50 and Y52 in CDR H2 provide hydrophobic interactions with the RBD (Fig. 4, E and F). CDR H3 also forms extensive interactions with the RBD (Fig. 4, G and H). The CDR H3 sequences of 38 antibodies that belong to this clonotype (17) (Fig. 4I) are highly conserved, and all contain a disulfide bond between V_H C97 and C100b, with four relatively small residues (G, S, T) in-between (Fig. 4, I, G and H). V_H D100d is also conserved (Fig. 4I), forming H-bonds with S477 and T478 (Fig. 4, G and H). In addition, the conserved V_H P95 and F100f (Fig. 4I) stack with RBD-F486 together with V_H W50, V_L Y91, and V_L W96 (Fig. 4, G and H). While E484 is often an important residue for antibody binding on the ridge region, here it is 5 Å distant from the antibodies and mutations at this site have not been reported as being sensitive for VH1-58 antibodies.

Thousands of anti-SARS-CoV-2 mAbs were isolated before the VOCs started to emerge (17), many of which are highly potent but with varying sensitivity to VOCs. Here, we characterized the antibody response to the RBD after SARS-CoV-2 Beta infection to provide insights into diverging and converging features of antibodies elicited by this lineage compared to wildtype-elicited antibodies.

Recently, the highly mutated Omicron variant has further increased the complexity of SARS-CoV-2 cross-variant immunity and resembles Beta as an antigenically distant VOC. Based on their shared RBD mutations, we hypothesized that some Beta-elicited mAbs also bind Omicron. Accordingly, VH3-53 mAb CS23, which binds the shared mutated residues N417 and Y501, showed comparable binding to Omicron and Beta (Fig. 4J). In contrast, Y501-dependent VH4-39 antibodies CS43 and CS170 did not bind to Omicron, suggesting other mutations in Omicron impede binding of this clonotype. Similarly, VH1-58 mAbs CS44 and CS102 also showed a drastic reduction in affinity to Omicron (Fig. 4J), suggesting that Omicron may not be efficiently neutralized by this public clonotype that exhibits ultra-high potency and high resistance to VOCs Alpha, Beta, Gamma and Delta (26). These findings emphasize the antigenic complexity and high temporal dynamics defining antibody immunity against SARS-CoV-2 in the context of ongoing antigenic drift, and provide insights for next-generation vaccine design and antibody therapeutics. For example, simultaneous or sequential immunization with vaccines based on diverse RBD sequences could be evaluated for superiority in induction of cross-variant immunity. While large-scale production of novel vaccine candidates based on the Omicron sequence have been initiated, those based on the Beta sequence already show promising cross-variant antibody titers in pre-clinical studies (29, 30), which led to the subsequent initiation of a phase II/III clinical trial. These clinical trials should be complemented by studies of the immune response against recent and future SARS-CoV-2 variants including Delta and Omicron, which are currently dominating global infections.

REFERENCES AND NOTES

- W. Dejnirattisai, D. Zhou, P. Supasa, C. Liu, A. J. Mentzer, H. M. Ginn, Y. Zhao, H. M. E. Duyvesteyn, A. Tuekprakhon, R. Nutalai, B. Wang, C. López-Camacho, J. Slon-Campos, T. S. Walter, D. Skelly, S. A. Costa Clemens, F. G. Naveca, V. Nascimento, F. Nascimento, C. Fernandes da Costa, P. C. Resende, A. Pauvolid-Correia, M. M. Siqueira, C. Dold, R. Levin, T. Dong, A. J. Pollard, J. C. Knight, D. Crook, T. Lambe, E. Clutterbuck, S. Bibi, A. Flaxman, M. Bittaye, S. Belij-Rammerstorfer, S. C. Gilbert, M. W. Carroll, P. Klenerman, E. Barnes, S. J. Dunachie, N. G. Paterson, M. A. Williams, D. R. Hall, R. J. G. Hulswit, T. A. Bowden, E. E. Fry, J. Mongkolsapaya, J. Ren, D. I. Stuart, G. R. Scratton, Antibody evasion by the P.1 strain of SARS-CoV-2. *Cell* **184**, 2939–2954.e9 (2021). doi:[10.1016/j.cell.2021.03.055](https://doi.org/10.1016/j.cell.2021.03.055) Medline
- P. Wang, M. S. Nair, L. Liu, S. Iketani, Y. Luo, Y. Guo, M. Wang, J. Yu, B. Zhang, P. D. Kwong, B. S. Graham, J. R. Mascola, J. Y. Chang, M. T. Yin, M. Sobieszczyn, C. A. Kyratsous, L. Shapiro, Z. Sheng, Y. Huang, D. D. Ho, Antibody resistance of SARS-CoV-2 variants B.1.351 and B.1.1.7. *Nature* **593**, 130–135 (2021). doi:[10.1038/s41586-021-03398-2](https://doi.org/10.1038/s41586-021-03398-2) Medline
- M. Hoffmann, P. Arora, R. Groß, A. Seidel, B. F. Hörnich, A. S. Hahn, N. Krüger, L. Graichen, H. Hofmann-Winkler, A. Kempf, M. S. Winkler, S. Schulz, H.-M.

- Jäck, B. Jahrsdörfer, H. Schrezenmeier, M. Müller, A. Kleger, J. Münch, S. Pöhlmann, SARS-CoV-2 variants B.1.351 and P.1 escape from neutralizing antibodies. *Cell* **184**, 2384–2393.e12 (2021). [doi:10.1016/j.cell.2021.03.036](https://doi.org/10.1016/j.cell.2021.03.036) Medline
- M. Hoffmann, H. Hofmann-Winkler, N. Krüger, A. Kempf, I. Nehlmeier, L. Graichen, P. Arora, A. Sidarovitch, A.-S. Moldenhauer, M. S. Winkler, S. Schulz, H.-M. Jäck, M. V. Stankov, G. M. N. Behrens, S. Pöhlmann, SARS-CoV-2 variant B.1.617 is resistant to bamlanivimab and evades antibodies induced by infection and vaccination. *Cell Rep.* **36**, 109415 (2021). [doi:10.1016/j.celrep.2021.109415](https://doi.org/10.1016/j.celrep.2021.109415) Medline
- D. Planas, T. Bruel, L. Grzelak, F. Guivel-Benhassine, I. Staropoli, F. Porrot, C. Planchais, J. Buchrieser, M. M. Rajah, E. Bishop, M. Albert, F. Donati, M. Prot, S. Behillil, V. Enouf, M. Maquart, M. Smati-Lafarge, E. Varon, F. Schortgen, L. Yahyaoui, M. Gonzalez, J. De Sèze, H. Pérez, D. Veyer, A. Sève, E. Simon-Lorière, S. Fafi-Kremer, K. Stefic, H. Mouquet, L. Hocqueloux, S. van der Werf, T. Prazuck, O. Schwartz, Sensitivity of infectious SARS-CoV-2 B.1.1.7 and B.1.351 variants to neutralizing antibodies. *Nat. Med.* **27**, 917–924 (2021). [doi:10.1038/s41591-021-01318-5](https://doi.org/10.1038/s41591-021-01318-5) Medline
- D. Zhou, W. Dejnirattisai, P. Supasa, C. Liu, A. J. Mentzer, H. M. Ginn, Y. Zhao, H. M. E. Duyvesteyn, A. Tuekprakhon, R. Nutalai, B. Wang, G. C. Paesen, C. Lopez-Camacho, J. Slon-Campos, B. Hallis, N. Coombes, K. Bewley, S. Charlton, T. S. Walter, D. Skelly, S. F. Lumley, C. Dold, R. Levin, T. Dong, A. J. Pollard, J. C. Knight, D. Crook, T. Lambe, E. Clutterbuck, S. Bibi, A. Flaxman, M. Bittaye, S. Bellj-Rammerstorfer, S. Gilbert, W. James, M. W. Carroll, P. Klenerman, E. Barnes, S. J. Dunachie, E. E. Fry, J. Mongkolsapaya, J. Ren, D. I. Stuart, G. R. Screaton, Evidence of escape of SARS-CoV-2 variant B.1.351 from natural and vaccine-induced sera. *Cell* **184**, 2348–2361.e6 (2021). [doi:10.1016/j.cell.2021.02.037](https://doi.org/10.1016/j.cell.2021.02.037) Medline
- M. Widera, A. Wilhelm, S. Hoehl, C. Pallas, N. Kohmer, T. Wolf, H. F. Rabenau, V. M. Corman, C. Drosten, M. J. G. T. Vehreschild, U. Goetsch, R. Gottschalk, S. Ciesek, Limited neutralization of authentic severe acute respiratory syndrome coronavirus 2 variants carrying E484K in vitro. *J. Infect. Dis.* **224**, 1109–1114 (2021). [doi:10.1093/infdis/jiab355](https://doi.org/10.1093/infdis/jiab355) Medline
- M. Rapp, Y. Guo, E. R. Reddem, J. Yu, L. Liu, P. Wang, G. Cerutti, P. Katsamba, J. S. Bimela, F. A. Bahna, S. M. Manneppalli, B. Zhang, P. D. Kwong, Y. Huang, D. D. Ho, L. Shapiro, Z. Sheng, Modular basis for potent SARS-CoV-2 neutralization by a prevalent VH1-2-derived antibody class. *Cell Rep.* **35**, 108950 (2021). [doi:10.1016/j.celrep.2021.108950](https://doi.org/10.1016/j.celrep.2021.108950) Medline
- M. Yuan, D. Huang, C. D. Lee, N. C. Wu, A. M. Jackson, X. Zhu, H. Liu, L. Peng, M. J. van Gils, R. W. Sanders, D. R. Burton, S. M. Reincke, H. Prüss, J. Kreye, D. Nemazee, A. B. Ward, I. A. Wilson, Structural and functional ramifications of antigenic drift in recent SARS-CoV-2 variants. *Science* **373**, 818–823 (2021). [doi:10.1126/science.abh1139](https://doi.org/10.1126/science.abh1139) Medline
- C. O. Barnes, C. A. Jette, M. E. Abernathy, K. A. Dam, S. R. Esswein, H. B. Gristick, A. G. Malyutin, N. G. Sharaf, K. E. Huey-Tubman, Y. E. Lee, D. F. Robbiani, M. C. Nussenzweig, A. P. West Jr., P. J. Bjorkman, SARS-CoV-2 neutralizing antibody structures inform therapeutic strategies. *Nature* **588**, 682–687 (2020). [doi:10.1038/s41586-020-2852-1](https://doi.org/10.1038/s41586-020-2852-1) Medline
- D. Geers, M. C. Shamier, S. Bogers, G. den Hartog, L. Gommers, N. N. Nieuwkoop, K. S. Schmitz, L. C. Rijsbergen, J. A. T. van Osch, E. Dijkhuizen, G. Smits, A. Comvalius, D. van Mourik, T. G. Caniels, M. J. van Gils, R. W. Sanders, B. B. Oude Munnink, R. Molenkamp, H. J. de Jager, B. L. Haagmans, R. L. de Swart, M. P. G. Koopmans, R. S. van Binnendijk, R. D. de Vries, C. H. Geurts van Kessel, SARS-CoV-2 variants of concern partially escape humoral but not T cell responses in COVID-19 convalescent donors and vaccine recipients. *Sci. Immunol.* **6**, eabj1750 (2021). [doi:10.1126/sciimmunol.abj1750](https://doi.org/10.1126/sciimmunol.abj1750) Medline
- C. Lucas, C. B. F. Vogels, I. Yildirim, J. E. Rothman, P. Lu, V. Monteiro, J. R. Gehlhausen, M. Campbell, J. Silva, A. Tabachnikova, M. A. Peña-Hernandez, M. C. Muenker, M. I. Breban, J. R. Fauver, S. Mohanty, J. Huang, A. C. Shaw, A. I. Ko, S. B. Omer, N. D. Grubaugh, A. Iwasaki, I. Ott, A. Watkins, C. Kalinich, T. Alpert, Yale SARS-CoV-2 Genomic Surveillance Initiative, Impact of circulating SARS-CoV-2 variants on mRNA vaccine-induced immunity. *Nature* **600**, 523–529 (2021). [doi:10.1038/s41586-021-04085-y](https://doi.org/10.1038/s41586-021-04085-y) Medline
- M. Cevik, N. D. Grubaugh, A. Iwasaki, P. Openshaw, COVID-19 vaccines: Keeping pace with SARS-CoV-2 variants. *Cell* **184**, 5077–5081 (2021). [doi:10.1016/j.cell.2021.09.010](https://doi.org/10.1016/j.cell.2021.09.010) Medline
- E. Cameroni, J. E. Bowen, L. E. Rosen, C. Saliba, S. K. Zepeda, K. Culap, D. Pinto, L. A. VanBlargan, A. De Marco, J. di Julio, F. Zatta, H. Kaiser, J. Noack, N. Farhat, N. Czudnochowski, C. Havenar-Daughton, K. R. Sprouse, J. R. Dillen, A. E. Powell, A. Chen, C. Maher, L. Yin, D. Sun, L. Soriaga, J. Bassi, C. Silacci-Fregnini, C. Gustafsson, N. M. Franko, J. Logue, N. T. Iqbal, I. Mazzitelli, J. Geffner, R. Grifantini, H. Chu, A. Gori, A. Riva, O. Giannini, A. Ceschi, P. Ferrari, P. E. Cippà, A. Franzetti-Pellanda, C. Garzoni, P. J. Halfmann, Y. Kawaoka, C. Hebner, L. A. Purcell, L. Piccoli, M. S. Pizzuto, A. C. Walls, M. S. Diamond, A. Telenti, H. W. Virgin, A. Lanzavecchia, G. Snell, D. Veesler, D. Corti, Broadly neutralizing antibodies overcome SARS-CoV-2 Omicron antigenic shift. *Nature* (2021). [doi:10.1038/s41586-021-04386-2](https://doi.org/10.1038/s41586-021-04386-2) Medline
- J. Kreye, N. K. Wenke, M. Chayka, J. Leubner, R. Murugan, N. Maier, B. Jurek, L.-T. Ly, D. Brandl, B. R. Rost, A. Stumpf, P. Schulz, H. Radbruch, A. E. Hauser, F. Pache, A. Meisel, L. Harms, F. Paul, U. Dirnagl, C. Garner, D. Schmitz, H. Wardemann, H. Prüss, Human cerebrospinal fluid monoclonal N-methyl-D-aspartate receptor autoantibodies are sufficient for encephalitis pathogenesis. *Brain* **139**, 2641–2652 (2016). [doi:10.1093/brain/aww208](https://doi.org/10.1093/brain/aww208) Medline
- T. Tiller, E. Meffre, S. Yurasov, M. Tsuji, M. C. Nussenzweig, H. Wardemann, Efficient generation of monoclonal antibodies from single human B cells by single cell RT-PCR and expression vector cloning. *J. Immunol. Methods* **329**, 112–124 (2008). [doi:10.1016/j.jim.2007.09.017](https://doi.org/10.1016/j.jim.2007.09.017) Medline
- M. I. J. Raybould, A. Kovaltsuk, C. Marks, C. M. Deane, CoV-AbDab: The coronavirus antibody database. *Bioinformatics* **37**, 734–735 (2021). [doi:10.1093/bioinformatics/btaa739](https://doi.org/10.1093/bioinformatics/btaa739) Medline
- C. Kreer, M. Zehner, T. Weber, M. S. Ercanoglu, L. Gieselmann, C. Rohde, S. Halwe, M. Korenkov, P. Schommers, K. Vanshylla, V. Di Cristanziano, H. Janicki, R. Brinker, A. Ashurov, V. Krähling, A. Kupke, H. Cohen-Dvashi, M. Koch, J. M. Eckert, S. Lederer, N. Pfeifer, T. Wolf, M. J. G. T. Vehreschild, C. Wendtner, R. Diskin, H. Gruell, S. Becker, F. Klein, Longitudinal isolation of potent near-germline SARS-CoV-2-neutralizing antibodies from COVID-19 patients. *Cell* **182**, 1663–1673 (2020). [doi:10.1016/j.cell.2020.08.046](https://doi.org/10.1016/j.cell.2020.08.046) Medline
- J. Kreye, S. M. Reincke, H.-C. Kornau, E. Sánchez-Sendin, V. M. Corman, H. Liu, M. Yuan, N. C. Wu, X. Zhu, C. D. Lee, J. Trimpert, M. Höltje, K. Dietert, L. Stöffler, N. von Wardenburg, S. van Hoof, M. A. Homeyer, J. Hoffmann, A. Abdalgawad, A. D. Gruber, L. D. Bertzbach, D. Vladimirova, L. Y. Li, P. C. Barthel, K. Skriner, A. C. Hocke, S. Hippensiel, M. Witzenrath, N. Suttorp, F. Kurth, C. Franke, M. Endres, D. Schmitz, L. M. Jeworowski, A. Richter, M. L. Schmidt, T. Schwarz, M. A. Müller, C. Drosten, D. Wendisch, L. E. Sander, N. Osterrieder, I. A. Wilson, H. Prüss, A therapeutic non-self-reactive SARS-CoV-2 antibody protects from lung pathology in a COVID-19 hamster model. *Cell* **183**, 1058–1069.e19 (2020). [doi:10.1016/j.cell.2020.09.049](https://doi.org/10.1016/j.cell.2020.09.049) Medline
- D. F. Robbiani, C. Gaebler, F. Muecksch, J. C. C. Lorenzi, Z. Wang, A. Cho, M. Agudelo, C. O. Barnes, A. Gazumyan, S. Finkin, T. Häggglöf, T. Y. Oliveira, C. Viant, A. Hurley, H.-H. Hoffmann, K. G. Millard, R. G. Kost, M. Cipolla, K. Gordon, F. Bianchini, S. T. Chen, V. Ramos, R. Patel, J. Dizon, I. Shimeliovich, P. Mendoza, H. Hartweger, L. Nogueira, M. Pack, J. Horowitz, F. Schmidt, Y. Weisblum, E. Michailidis, A. W. Ashbrook, E. Waltari, J. E. Pak, K. E. Huey-Tubman, N. Koranda, P. R. Hoffman, A. P. West Jr., C. M. Rice, T. Hatziaannou, P. J. Bjorkman, P. D. Bieniasz, M. Caskey, M. C. Nussenzweig, Convergent antibody responses to SARS-CoV-2 in convalescent individuals. *Nature* **584**, 437–442 (2020). [doi:10.1038/s41586-020-2456-9](https://doi.org/10.1038/s41586-020-2456-9) Medline
- Z. Wang, F. Schmidt, Y. Weisblum, F. Muecksch, C. O. Barnes, S. Finkin, D. Schaefer-Babajew, M. Cipolla, C. Gaebler, J. A. Lieberman, T. Y. Oliveira, Z. Yang, M. E. Abernathy, K. E. Huey-Tubman, A. Hurley, M. Turroja, K. A. West, K. Gordon, K. G. Millard, V. Ramos, J. Da Silva, J. Xu, R. A. Colbert, R. Patel, J. Dizon, C. Unson-O'Brien, I. Shimeliovich, A. Gazumyan, M. Caskey, P. J. Bjorkman, R. Casellas, T. Hatziaannou, P. D. Bieniasz, M. C. Nussenzweig, mRNA vaccine-elicited antibodies to SARS-CoV-2 and circulating variants. *Nature* **592**, 616–622 (2021). [doi:10.1038/s41586-021-03324-6](https://doi.org/10.1038/s41586-021-03324-6) Medline
- C. O. Barnes, A. P. West Jr., K. E. Huey-Tubman, M. A. G. Hoffmann, N. G.

- Sharaf, P. R. Hoffman, N. Koranda, H. B. Gristick, C. Gaebler, F. Muecksch, J. C. Lorenzi, S. Finkin, T. Hägglöf, A. Hurley, K. G. Millard, Y. Weisblum, F. Schmidt, T. Hatzloannou, P. D. Bieniasz, M. Caskey, D. F. Robbiani, M. C. Nuszenzweig, P. J. Bjorkman, Structures of human antibodies bound to SARS-CoV-2 spike reveal common epitopes and recurrent features of antibodies. *Cell* **182**, 828–842.e16 (2020). [doi:10.1016/j.cell.2020.06.025](https://doi.org/10.1016/j.cell.2020.06.025) Medline
23. N. C. Wu, M. Yuan, H. Liu, C. D. Lee, X. Zhu, S. Bangaru, J. L. Torres, T. G. Caniels, P. J. M. Brouwer, M. J. van Gils, R. W. Sanders, A. B. Ward, I. A. Wilson, An alternative binding mode of IGHV3-53 antibodies to the SARS-CoV-2 receptor binding domain. *Cell Rep.* **33**, 108274 (2020). [doi:10.1016/j.celrep.2020.108274](https://doi.org/10.1016/j.celrep.2020.108274) Medline
24. M. Yuan, H. Liu, N. C. Wu, C. D. Lee, X. Zhu, F. Zhao, D. Huang, W. Yu, Y. Hua, H. Tien, T. F. Rogers, E. Landais, D. Sok, J. G. Jardine, D. R. Burton, I. A. Wilson, Structural basis of a shared antibody response to SARS-CoV-2. *Science* **369**, 1119–1123 (2020). [doi:10.1126/science.abd2321](https://doi.org/10.1126/science.abd2321) Medline
25. M. Yuan, H. Liu, N. C. Wu, I. A. Wilson, Recognition of the SARS-CoV-2 receptor binding domain by neutralizing antibodies. *Biochem. Biophys. Res. Commun.* **538**, 192–203 (2021). [doi:10.1016/j.bbrc.2020.10.012](https://doi.org/10.1016/j.bbrc.2020.10.012) Medline
26. L. Wang, T. Zhou, Y. Zhang, E. S. Yang, C. A. Schramm, W. Shi, A. Pegu, O. K. Oloniniyi, A. R. Henry, S. Darko, S. R. Narpala, C. Hatcher, D. R. Martinez, Y. Tsybovsky, E. Phung, O. M. Abiona, A. Antia, E. M. Cale, L. A. Chang, M. Choe, K. S. Corbett, R. L. Davis, A. T. DiPiazza, I. J. Gordon, S. H. Hait, T. Hermanus, P. Kgagudi, F. Laboune, K. Leung, T. Liu, R. D. Mason, A. F. Nazzari, L. Novik, S. O’Connell, S. O’Dell, A. S. Olia, S. D. Schmidt, T. Stephens, C. D. Stringham, C. A. Talana, I.-T. Teng, D. A. Wagner, A. T. Widge, B. Zhang, M. Roederer, J. E. Ledgerwood, T. J. Ruckwardt, M. R. Gaudinski, P. L. Moore, N. A. Doria-Rose, R. S. Baric, B. S. Graham, A. B. McDermott, D. C. Douek, P. D. Kwong, J. R. Mascola, N. J. Sullivan, J. Misasi, Ultrapotent antibodies against diverse and highly transmissible SARS-CoV-2 variants. *Science* **373**, eabih1766 (2021). [doi:10.1126/science.abh1766](https://doi.org/10.1126/science.abh1766) Medline
27. W. Dejnirattisai, D. Zhou, H. M. Ginn, H. M. E. Duyvesteyn, P. Supasa, J. B. Case, Y. Zhao, T. S. Walter, A. J. Mentzer, C. Liu, B. Wang, G. C. Paesen, J. Slon-Campos, C. López-Camacho, N. M. Kafai, A. L. Bailey, R. E. Chen, B. Ying, C. Thompson, J. Bolton, A. Fyfe, S. Gupta, T. K. Tan, J. Gilbert-Jaramillo, W. James, M. Knight, M. W. Carroll, D. Skelly, C. Dold, Y. Peng, R. Levin, T. Dong, A. J. Pollard, J. C. Knight, P. Kleinerman, N. Temperton, D. R. Hall, M. A. Williams, N. G. Paterson, F. K. R. Bertram, C. A. Siebert, D. K. Clare, A. Howe, J. Radecke, Y. Song, A. R. Townsend, K. A. Huang, E. E. Fry, J. Mongkolsapaya, M. S. Diamond, J. Ren, D. I. Stuart, G. R. Screamton, The antigenic anatomy of SARS-CoV-2 receptor binding domain. *Cell* **184**, 2183–2200.e22 (2021). [doi:10.1016/j.cell.2021.02.032](https://doi.org/10.1016/j.cell.2021.02.032) Medline
28. M. A. Tortorici, M. Beltramo, F. A. Lempp, D. Pinto, H. V. Dang, L. E. Rosen, M. McCallum, J. Bowen, A. Minola, S. Jaconi, F. Zatta, A. De Marco, B. Guarino, S. Bianchi, E. J. Lauron, H. Tucker, J. Zhou, A. Peter, C. Havenar-Daughton, J. A. Wojciechowsky, J. B. Case, R. E. Chen, H. Kaiser, M. Montiel-Ruiz, M. Meury, N. Czudnochowski, R. Spreafico, J. Dillen, C. Ng, N. Sprugasci, K. Culap, F. Benigni, R. Abdelnabi, S. C. Foo, M. A. Schmid, E. Cameroni, A. Riva, A. Gabrieli, M. Galli, M. S. Pizzuto, J. Neyts, M. S. Diamond, H. W. Virgin, G. Snell, D. Corti, K. Fink, D. Veesler, Ultrapotent human antibodies protect against SARS-CoV-2 challenge via multiple mechanisms. *Science* **370**, 950–957 (2020). [doi:10.1126/science.abe3354](https://doi.org/10.1126/science.abe3354) Medline
29. A. J. Spencer *et al.*, The ChAdOx1 vectored vaccine, AZD2816, induces strong immunogenicity against SARS-CoV-2 Beta (B.1.351) and other variants of concern in preclinical studies. *bioRxiv*, 2021.06.08.447308 (2021).
30. B. Ying, B. Whitener, L. A. VanBlargan, A. O. Hassan, S. Shrihari, C. Y. Liang, C. E. Karl, S. Mackin, R. E. Chen, N. M. Kafai, S. H. Wilks, D. J. Smith, J. M. Carreño, G. Singh, F. Krammer, A. Carfi, S. M. Elbashir, D. K. Edwards, L. B. Thackray, M. S. Diamond, Protective activity of mRNA vaccines against ancestral and variant SARS-CoV-2 strains. *Sci. Transl. Med.* eabm3302 (2021). [doi:10.1126/scitranslmed.abm3302](https://doi.org/10.1126/scitranslmed.abm3302) Medline
31. S. D. Boyd, B. A. Gaëta, K. J. Jackson, A. Z. Fire, E. L. Marshall, J. D. Merker, J. M. Maniar, L. N. Zhang, B. Sahaf, C. D. Jones, B. B. Simen, B. Hanczaruk, K. D. Nguyen, K. C. Nadeau, M. Egholm, D. B. Miklos, J. L. Zehnder, A. M. Collins, Individual variation in the germline Ig gene repertoire inferred from variable region gene rearrangements. *J. Immunol.* **184**, 6986–6992 (2010). [doi:10.4049/jimmunol.1000445](https://doi.org/10.4049/jimmunol.1000445) Medline
32. S. M. Reincke, H. Prüss, J. Kreye, Brain antibody sequence evaluation (BASE): An easy-to-use software for complete data analysis in single cell immunoglobulin cloning. *BMC Bioinformatics* **21**, 446 (2020). [doi:10.1186/s12859-020-03741-w](https://doi.org/10.1186/s12859-020-03741-w) Medline
33. Z. Gu, L. Gu, R. Eils, M. Schlesner, B. Brors, circdIle implements and enhances circular visualization in R. *Bioinformatics* **30**, 2811–2812 (2014). [doi:10.1093/bioinformatics/btu393](https://doi.org/10.1093/bioinformatics/btu393) Medline
34. D. Hillus, T. Schwarz, P. Tober-Lau, K. Vanshylla, H. Hastor, C. Thibeault, S. Jentzsch, E. T. Helbig, L. J. Lippert, P. Tscheak, M. L. Schmidt, J. Riege, A. Solarek, C. von Kalle, C. Dang-Heine, H. Gruell, P. Kopankiewicz, N. Suttorp, C. Drosten, H. Bias, J. Seybold, F. Klein, F. Kurth, V. M. Corman, L. E. Sander, EICOV/COVIM Study Group, Safety, reactogenicity, and immunogenicity of homologous and heterologous prime-boost immunisation with ChAdOx1 nCoV-19 and BNT162b2: A prospective cohort study. *Lancet Respir. Med.* **9**, 1255–1265 (2021). [doi:10.1016/S2213-2600\(21\)00357-X](https://doi.org/10.1016/S2213-2600(21)00357-X) Medline
35. W. T. Harvey, A. M. Carabelli, B. Jackson, R. K. Gupta, E. C. Thomson, E. M. Harrison, C. Ludden, R. Reeve, A. Rambaut, S. J. Peacock, D. L. Robertson; COVID-19 Genomics UK (COG-UK) Consortium, SARS-CoV-2 variants, spike mutations and immune escape. *Nat. Rev. Microbiol.* **19**, 409–424 (2021). [doi:10.1038/s41579-021-00573-0](https://doi.org/10.1038/s41579-021-00573-0) Medline
36. S. P. Otto, T. Day, J. Arino, C. Colijn, J. Dushoff, M. Li, S. Mechai, G. Van Domselaar, J. Wu, D. J. D. Earn, N. H. Ogden, The origins and potential future of SARS-CoV-2 variants of concern in the evolving COVID-19 pandemic. *Curr. Biol.* **31**, R918–R929 (2021). [doi:10.1016/j.cub.2021.06.049](https://doi.org/10.1016/j.cub.2021.06.049) Medline
37. R. Wölfel, V. M. Corman, W. Guggemos, M. Seilmaier, S. Zange, M. A. Müller, D. Niemeyer, T. C. Jones, P. Vollmar, C. Rothe, M. Hoelscher, T. Bleicker, S. Brünink, J. Schneider, R. Ehmann, K. Zwirglmaier, C. Drosten, C. Wendtner, Virological assessment of hospitalized patients with COVID-2019. *Nature* **581**, 465–469 (2020). [doi:10.1038/s41586-020-2196-x](https://doi.org/10.1038/s41586-020-2196-x) Medline
38. D. C. Ekiert, R. H. E. Friesen, G. Bhabha, T. Kwaks, M. Jongeneelen, W. Yu, C. Ophorst, F. Cox, H. J. W. M. Korse, B. Brandenburg, R. Vogels, J. P. J. Brakenhoff, R. Kompier, M. H. Koldijk, L. A. H. M. Cornelissen, L. L. M. Poon, M. Peiris, W. Koudstaal, I. A. Wilson, J. Goudsmit, A highly conserved neutralizing epitope on group 2 influenza A viruses. *Science* **333**, 843–850 (2011). [doi:10.1126/science.1204839](https://doi.org/10.1126/science.1204839) Medline
39. H. Liu, M. Yuan, D. Huang, S. Bangaru, F. Zhao, C. D. Lee, L. Peng, S. Barman, X. Zhu, D. Nemazee, D. R. Burton, M. J. van Gils, R. W. Sanders, H.-C. Kornau, S. M. Reincke, H. Prüss, J. Kreye, N. C. Wu, A. B. Ward, I. A. Wilson, A combination of cross-neutralizing antibodies synergizes to prevent SARS-CoV-2 and SARS-CoV pseudovirus infection. *Cell Host Microbe* **29**, 806–818.e6 (2021). [doi:10.1016/j.chom.2021.04.005](https://doi.org/10.1016/j.chom.2021.04.005) Medline
40. Z. Otwinowski, W. Minor, Processing of X-ray diffraction data collected in oscillation mode. *Methods Enzymol.* **276**, 307–326 (1997). [doi:10.1016/S0076-6879\(97\)76066-X](https://doi.org/10.1016/S0076-6879(97)76066-X)
41. A. J. McCoy, R. W. Grosse-Kunstleve, P. D. Adams, M. D. Winn, L. C. Storoni, R. J. Read, Phaser crystallographic software. *J. Appl. Crystallogr.* **40**, 658–674 (2007). [doi:10.1107/S0021889807021206](https://doi.org/10.1107/S0021889807021206) Medline
42. P. Emsley, B. Lohkamp, W. G. Scott, K. Cowtan, Features and development of Coot. *Acta Crystallogr. D Biol. Crystallogr.* **66**, 486–501 (2010). [doi:10.1107/S0907444910007493](https://doi.org/10.1107/S0907444910007493) Medline
43. P. D. Adams, P. V. Afonine, G. Bunkóczki, V. B. Chen, I. W. Davis, N. Echols, J. J. Headd, L.-W. Hung, G. J. Kapral, R. W. Grosse-Kunstleve, A. J. McCoy, N. W. Moriarty, R. Oeffner, R. J. Read, D. C. Richardson, J. S. Richardson, T. C. Terwilliger, P. H. Zwart, PHENIX: A comprehensive Python-based system for macromolecular structure solution. *Acta Crystallogr. D Biol. Crystallogr.* **66**, 213–221 (2010). [doi:10.1107/S0907444909052925](https://doi.org/10.1107/S0907444909052925) Medline
44. E. Krissinel, K. Henrick, Inference of macromolecular assemblies from crystalline state. *J. Mol. Biol.* **372**, 774–797 (2007). [doi:10.1016/j.jmb.2007.05.022](https://doi.org/10.1016/j.jmb.2007.05.022) Medline
45. V. B. Chen, W. B. Arendall 3rd, J. J. Headd, D. A. Keedy, R. M. Immormino, G. J. Kapral, L. W. Murray, J. S. Richardson, D. C. Richardson, MolProbity: All-atom structure validation for macromolecular crystallography. *Acta Crystallogr. D Biol. Crystallogr.* **66**,

ACKNOWLEDGMENTS

We thank all study participants who devoted samples and time to our research, Dr. Kim Stahlberg and Meilan Zuo for patient recruitment, Stefanie Bandura, Matthias Sillmann, Doreen Brandl, Patricia Tscheak, and Sabine Engl for excellent technical assistance, and Dr. Marcel A. Müller and Dr. Daniela Niemeyer for support with BSL3 work. We acknowledge BIAFFIN GmbH & Co. KG (Kassel, Germany) for performance of SPR measurements and the Flow and Mass Cytometry Core Facility at Charité-Universitätsmedizin Berlin for support with single-cell sorting. We thank Robyn Stanfield for assistance in data collection, Fangzhu Zhao for assistance in the biolayer interferometry binding assay, and the staff of Advanced Light Source beamline 5.0.1 and Stanford Synchrotron Radiation Laboratory (SSRL) beamline 12-1 for assistance. SARS-CoV-2 RBD variants antigens for sera testing were kindly provided by InVivo BioTech Services GmbH (Hennigsdorf, Germany) to the Seramun Diagnostica GmbH (Heidesee, Germany). S.M.R. and J.K. are participants in the BIH-Charité Junior Clinician Scientist Program and V.M.C is supported by Berlin Institute of Health (BIH) Charité Clinician Scientist program both funded by Charité – Universitätsmedizin Berlin and the Berlin Institute of Health. **Funding:** This work was supported by the Bill and Melinda Gates Foundation INV-004923 (I.A.W.), by the Bavarian State Ministry of Science and the Arts; University Hospital; Ludwig-Maximilians-Universität Munich; German Ministry for Education and Research (Proj. Nr.: 01KI20271, M.H.; Connect-Generate 01GM1908D, H.P.); by the Helmholtz Association (ExNet-0009-Phase2-3, D.S.; HIL-A03, H.P.), by the German Research Foundation (DFG) (PR1274/3-1 and PR1274/5-1, H.P.), and by the Austrian Science Fund (FWF J4157-B30, M.R.). Parts of the work was funded by the European Union's Horizon 2020 research and innovation program through project RECOVER (GA101003589) to C.D.; the German Ministry of Research through the projects VARIPath (01KI2021) to V.M.C and NaFoUniMedCovid19 - COVIM, FKZ: 01KX2021 to C.D., and V.M.C. This research used resources of the Advanced Light Source, which is a DOE Office of Science User Facility under contract number DE-AC02-05CH11231. Use of the SSRL, SLAC National Accelerator Laboratory, is supported by the U.S. Department of Energy, Office of Science, Office of Basic Energy Sciences under Contract No. DE-AC02-76SF00515. The SSRL Structural Molecular Biology Program is supported by the DOE Office of Biological and Environmental Research, and by the National Institutes of Health, National Institute of General Medical Sciences (including P41GM103393). **Author contributions:** Conceptualization: S.M.R., M.Y., H.-C.K., V.M.C., H.P., I.A.W., and J.K.; Patient recruitment and sample preparation: S.M.R., M.R., M.A.H., I.K., T.M.E., C.G., A.W., M.H., H.G., G.W., S.H., H.P., and J.K.; Antibody production: S.M.R., S.v.H., E.S.-S., M.R., S.E.B., H.F.R., M.A.H., L.S., D.K., N.v.W., and J.K.; Antibody reactivity testing: H.-C.K.; Serological assays and neutralization testing: V.M.C., M.L.S., T.S., L.M.J., and C.D.; Protein production and crystallography: M.Y., W.Y., Y.H., and H.T.; Software: M.B., J.H., and S.M.R.; Resources: V.M.C., M.H., G.W., D.S., C.D., H.P., and I.A.W.; Writing – Original Draft: S.M.R., M.Y., H.-C.K., H.P., I.A.W., and J.K.; Writing – Review and Editing: all authors; Supervision: S.M.R., M.Y., H.-C.K., V.M.C., H.P., I.A.W., and J.K. **Competing interests:** The German Center for Neurodegenerative Diseases (DZNE) and Charité-Universitätsmedizin Berlin have filed a patent application on antibodies for the treatment of SARS-CoV-2 infection described in an earlier publication, on which S.M.R., H.-C.K., V.M.C., E.S.-S., H.P., and J.K. are named as inventors. V.M.C. is named together with Euroimmun GmbH on a patent application filed recently regarding the diagnostic of SARS-CoV-2 by antibody testing. **Data and materials availability:** X-ray coordinates and structure factors are deposited at the RCSB Protein Data Bank under accession codes 7SSP, 7SSQ and 7SSR. The amino acid sequences of the antibodies described in this study can be found in table S3. All requests for materials including antibodies, viruses, plasmids and proteins generated in this study should be directed to the corresponding authors. Materials will be made available for non-commercial usage. This work is licensed under a Creative Commons Attribution 4.0 International (CC

BY 4.0) license, which permits unrestricted use, distribution, and reproduction in any medium, provided the original work is properly cited. To view a copy of this license, visit <https://creativecommons.org/licenses/by/4.0/>. This license does not apply to figures/photos/artwork or other content included in the article that is credited to a third party; obtain authorization from the rights holder before using such material.

SUPPLEMENTARY MATERIALS

science.org/doi/10.1126/science.abm5835

Materials and Methods

Figs. S1 to S6

Tables S1 to S6

References (32–45)

29 September 2021; accepted 18 January 2022

Published online 25 January 2022

10.1126/science.abm5835

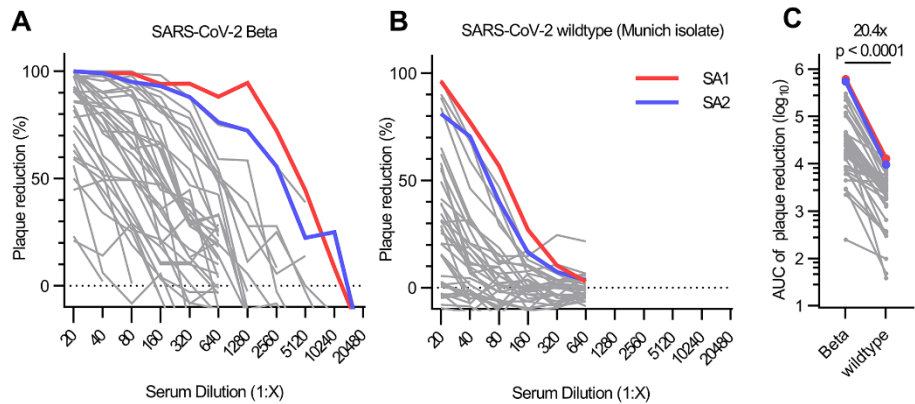


Fig. 1. Authentic virus neutralization of sera from individuals after infection with SARS-CoV-2 Beta. (A and B) Neutralizing activity of sera of patients infected with SARS-CoV-2 Beta variant was measured using a plaque-reduction neutralization assay with the indicated authentic virus. Results are given as reduction of plaque number at indicated serum dilutions. Patients SA1 and SA2 mounted the strongest antibody response, which are highlighted in red and blue, respectively. Means of duplicate measurements are shown. Values below zero indicate no plaque reduction. (C) Change in neutralization activity against SARS-CoV-2 Beta and wildtype SARS-CoV-2 based on area under the curve (AUC) calculations from authentic virus PRNT curves [shown in (A) and (B)]. Mean fold change is indicated above the p value. Statistical analysis was performed using a Wilcoxon matched-pairs signed-rank test with two-tailed p value.

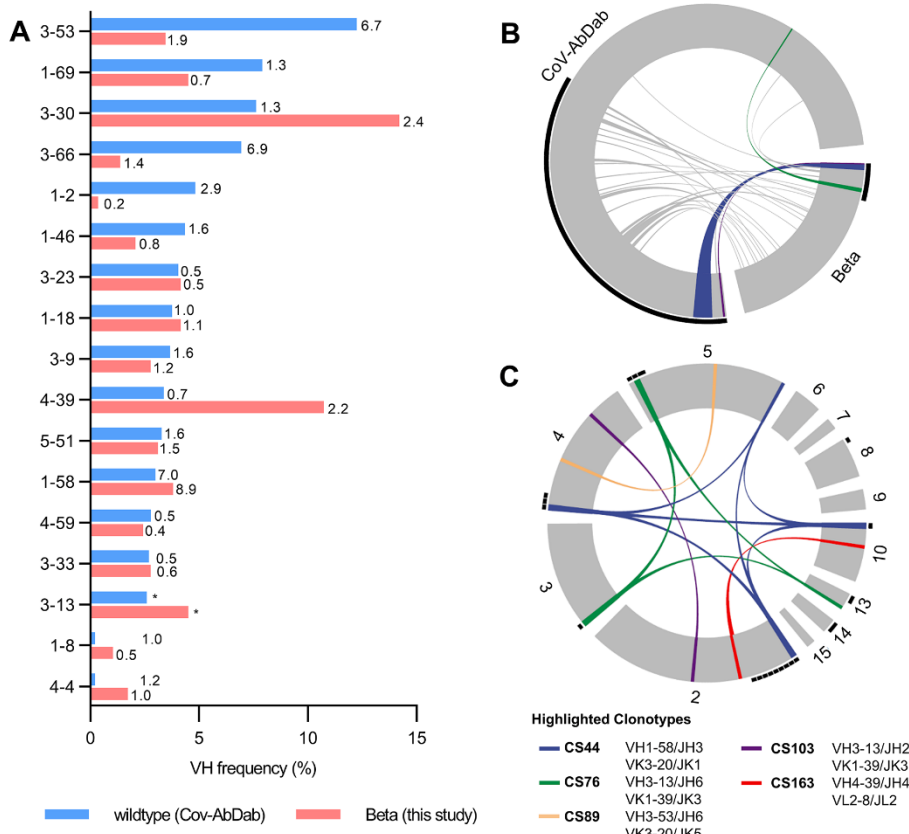


Fig. 2. Germline gene usage and clonotype analysis of Beta-elicited antibodies. (A) VH gene usage of 289 RBD Beta IgG mAbs from this study (red) is compared to 1037 wildtype RBD mAbs from 96 previously published studies (blue, CoV-AbDab) (17). Frequencies of mAbs encoded by each VH gene are shown as bars. Enrichment of indicated VH genes is compared to healthy individuals (31) with fold-enrichment shown as number next to bars. VH gene frequencies that were not reported in healthy individuals (31) are shown with asterisk (*). Only VH genes with a frequency of at least 2% in CoV-AbDab are shown and VH genes are ordered by frequency in CoV-AbDab. (B) Circos plot shows the relationship between 289 IgG mAbs from this study (Beta) and 1037 previously published human mAbs reactive to RBD (wildtype) from 96 studies (17). Interconnecting lines display clonotypes shared between both datasets, as defined by the usage of the same V and J gene on both Ig heavy and light chain. Thin black lines at the outer circle border indicate expanded clonotypes within the respective data set. (C) Circos plot displaying the 289 IgG mAbs from this study grouped per patient. Interconnecting colored lines indicate clonotypes found in more than one patient. Small black angles at the outer circle border indicate clonally expanded clones within one patient. [(B) and (C)] Colored interconnecting lines depict clonotypes found in more than one patient of our cohort.

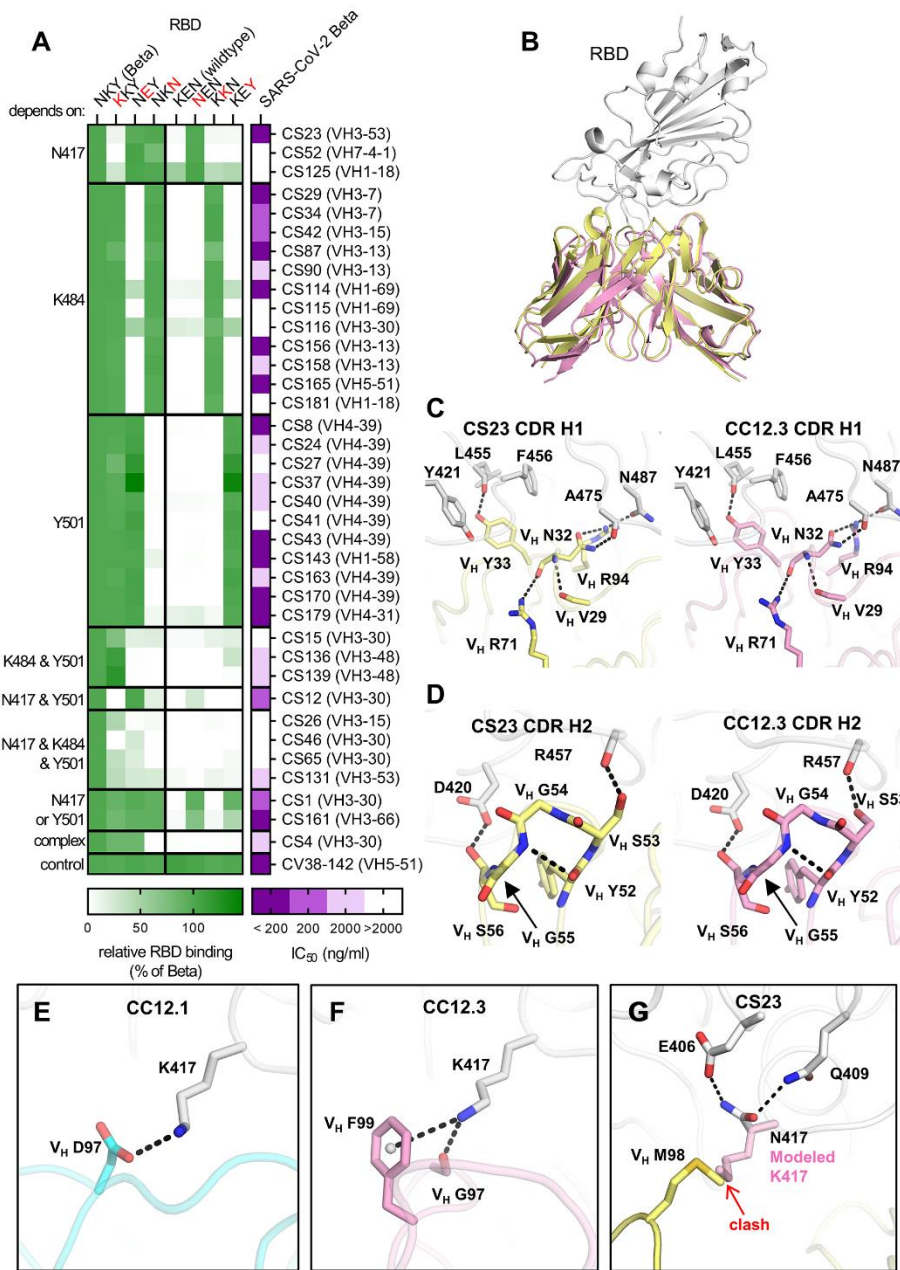


Fig. 3. Binding, neutralization and structures of Beta-specific antibodies. (A) Neutralization of indicated Beta-specific mAbs against authentic Beta virus is shown in purple. Binding to single point mutant RBD constructs with the indicated amino-acid residues at positions 417, 484 and 501 is shown in green, normalized to RBD Beta. (B to G) Structural comparison of VH3-53 mAbs between Beta-specific CS23 and wildtype-specific CC12.1 and CC12.3. (B) CC12.3 and CS23 adopt the same binding mode. The crystal structure of CC12.3 (pink) in complex with RBD (wildtype) was superimposed onto CS23 (yellow) in complex with RBD (Beta). Only the variable domains of the antibodies are shown for clarity. A small local conformational difference was observed between CS23-bound RBD Beta and CC12.3-bound wildtype RBD (191 C α , RMSD = 0.8 Å). (C and D) Comparison of the (C) CDR H1 ('NY' motif) and (D) CDR H2 ('SGGS' motif) between CS23 and CC12.3. (E to G) Structures of CDR H3 of (E) CC12.1, (F) CC12.3, and (G) CS23. A modeled side chain of K417 is shown as transparent pink sticks, which would be unfavorable for binding to CS23, where V_H M98 occupies this pocket. Structures of CC12.1 (PDB 6XC3, cyan), CC12.3 (PDB 6XC4, pink), and CS23 (this study, yellow) are used throughout this figure, and the RBD is shown in white. Hydrogen bonds, salt bridges or cation-π bonds are represented by black dashed lines.

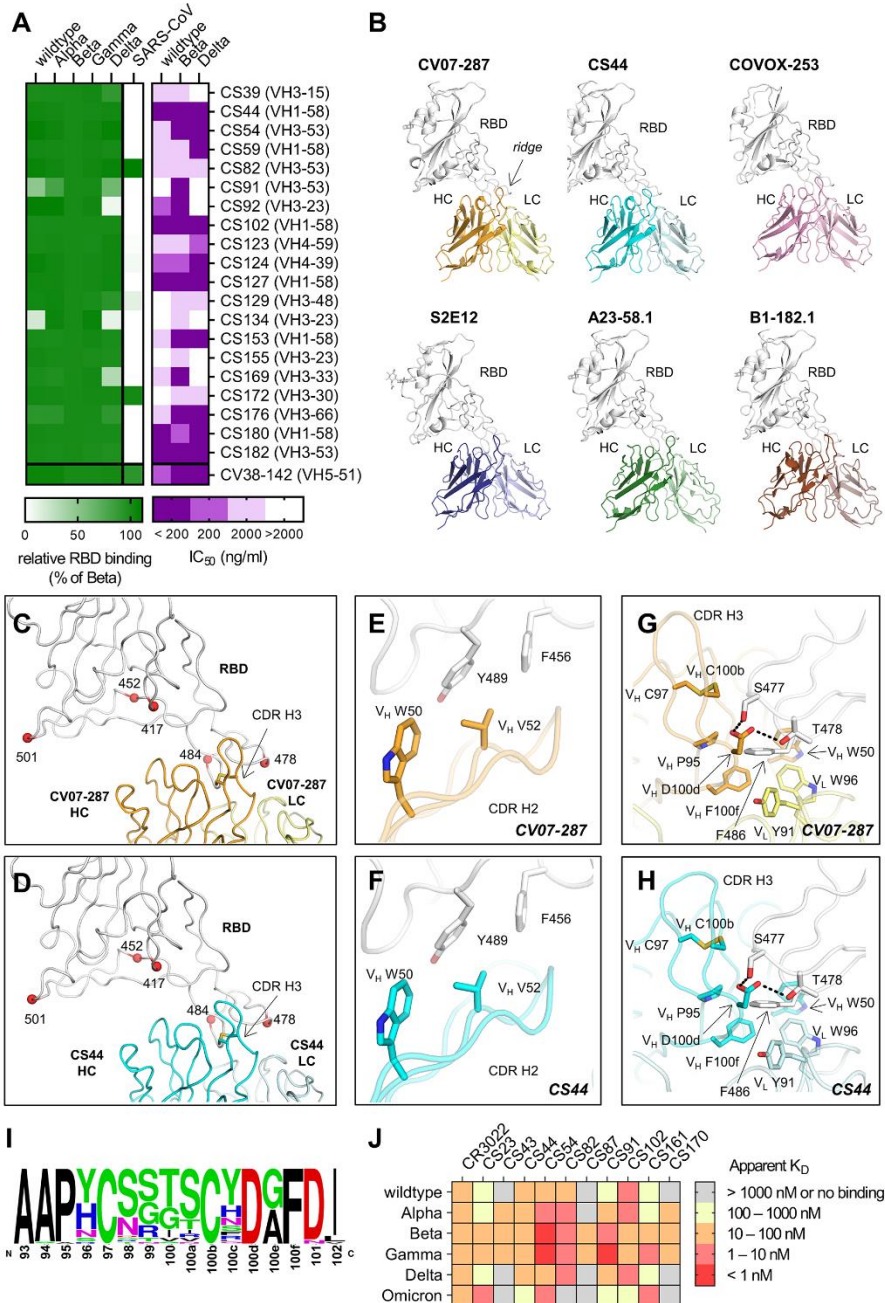


Fig. 4. Characterization of cross-reactive mAbs and crystal structures of CV07-287 and CS44. (A) Neutralization of cross-reactive antibodies against authentic Beta, Delta and wildtype virus is shown in purple. Binding to the indicated RBD constructs is shown in green, normalized to RBD Beta. (B) VH1-58 antibodies target SARS-CoV-2 RBD via the same binding mode. Crystal structures of CV07-287 in complex with wildtype RBD and CS44 in complex with RBD Beta are shown. COVA1-16 Fab that was used in the crystallization to form the crystal lattice is not shown for clarity. Structures of VH1-58 antibodies from other studies are shown for comparison, including COVOX-253 (PDB 7BEN), S2E12 (PDB 7K45), A23-58.1 (PDB 7LRT), and B1-182.1 (PDB 7MM0). All structures are shown in the same orientation, with the constant domains of the Fab omitted for clarity. The location of the ridge region of the RBD is indicated in the first panel. (C and D) Mutated residues in VOCs B.1.1.7 (Alpha), B.1.351 (Beta), B.1.617.2 (Delta), and P.1 (Gamma) variants are represented by red spheres. All of these residues are distant from VH1-58 antibodies (C) CV07-287 and (D) CS44, except for T478. The disulfide bond in each CDR H3 is shown as sticks. (E to H) Detailed interactions between the RBD and [ε and (G)] CV07-287, and [(F) and (H)] CS44, respectively. RBDs are shown in white, with heavy and light chains of CV07-287 in orange and yellow, and those of CS44 in cyan and light cyan, respectively. Interactions of CDR H2 are in (E) and (F), and those of CDR H3 are in (G) and (H). Hydrogen bonds are represented by black dashed lines. (I) Sequence logo of CDR H3 of VH1-58/VK3-20 antibodies. CDR H3 sequences of VH1-58/VK3-20 antibodies from COVID-19 patients (17) were aligned and analyzed with WebLogo. (J) Affinity of indicated Beta-elicited mAbs to RBD of indicated VOCs was determined by biolayer interferometry.